Energy 322 (2025) 135574

Contents lists available at ScienceDirect

Energy

journal homepage: www.elsevier.com/locate/energy

Experimental study and process evaluation of a graded utilization strategy for woody biomass: Integration of reductive catalytic fractionation, hydrodeoxygenation, and catalytic pyrolysis

Qian Qian [a], Zhongyang Luo [a,*], Feiting Miao [a], Caixia Song [a], Jingkang Shi [a], Liwen Du [a], Qingguo Zhou [a], Evgeny R. Naranov [b]

[a] State Key Laboratory of Clean Energy Utilization, Zhejiang University, Hangzhou, 310027, PR China
[b] A.V. Topchiev Institute of Petrochemical Synthesis RAS, Leninsky Avenue 29, 119991, Moscow, Russia

ARTICLE INFO

Keywords:
Reductive catalytic fractionation
Mild hydrodeoxygenation
Catalytic pyrolysis
Process modeling
Process evaluation

ABSTRACT

Complete conversion of lignocellulose into fuels and chemicals is significant yet challenging. This study proposes a novel graded utilization strategy for woody biomass, where reductive catalytic fractionation is followed by mild bio-oil hydrodeoxygenation for hydrocarbons generation and solid residue pyrolysis for alternative fuels and furfural production. Roles of metal-loaded alumina catalysts in H_2-free reductive catalytic fractionation were clarified, achieving aromatic monomer yields of ~39 wt%. Hexane pre-extraction of monomers before mild hydrodeoxygenation over Ru/Nb_2O_5 increased the hydrocarbon yield by 25 % relative to direct hydrodeoxygenation of crude aromatic bio-oils. Holocellulose-rich residues underwent catalytic pyrolysis using the same $NiMo/Al_2O_3$. Consequently, 10 %, 8 %, and 9 % of feedstock carbon are retained as hydrocarbons, furfural compounds, and other alternative fuels, respectively. Increasing ideal products yield and reducing solvent loading can significantly enhance system energy recovery. The estimated minimum fuel selling price aligns with the average retail gasoline price and could drop to $2.10 per gallon with an optimized solvent-to-biomass ratio. Meanwhile, the environmental benefits are substantial, not only reducing GHG emissions but also preventing burden shifting to other categories. This strategy offers a new pathway for co-producing fuels and chemicals from woody biomass, with future efforts needed to drive technological breakthroughs and mitigate commercialization risks.

1. Introduction

Extensive emissions of greenhouse gases resulting from industrial & anthropogenic activities have led to increasing global temperatures and shifting climatic conditions, sparking concerns for decades [1]. Biomass is expected to offer alternative solutions for combating climate change through diverse conversion technologies [2]. Lignocellulosic biomass, an abundant and sustainable non-food carbon source primarily composed of cellulose, hemicellulose, and lignin, offers significant potential to expand global production of renewable fuels and chemicals [3]. However, most biorefineries focus on the isolation, purification, conversion of carbohydrates, whereas lignin has seen limited high-value practical applications thus far [4]. Despite its rich benzene ring structure and associated aromatic properties, lignin holds significant potential for the production of value-added products [5]. However, native lignin is predisposed to undergo polycondensation under harsh reaction conditions, yielding chemically recalcitrant technical lignin that is difficult to convert and often ends up being burned as waste. It's crucial to develop innovative biorefining methods that fully harness the value of all lignocellulose components for enhancing overall profitability and sustainability [6].

Recently, the "lignin-first" biorefinery concept was proposed, prioritizing lignin availability while maximizing carbohydrate preservation. This approach offers a new solution for components separation, overcoming degradation barriers, and fully valorizing lignocellulose [7]. Reductive catalytic fractionation has emerged as a novel method, enabling high yield and selectivity in producing monophenol derivatives. Meanwhile, selective depolymerization of lignin into liquid intermediates allows carbohydrates to remain in solid form, thereby simplifying downstream processing [8]. Research on this technique has

* Corresponding author.
E-mail address: zyluo@zju.edu.cn (Z. Luo).

https://doi.org/10.1016/j.energy.2025.135574
Received 22 November 2024; Received in revised form 8 March 2025; Accepted 10 March 2025
Available online 11 March 2025

shown that the yield and selectivity of monophenols are highly dependent on factors such as feedstocks, solvents, and catalysts. Encouraging results have been achieved in obtaining high phenolic monomer yields using commercial Ni-Al_2O_3 pellets, which play a crucial role in hydrogenating reactive unsaturated side chains in lignin intermediates, thereby preventing their repolymerization into high-molecular-weight lignin [9]. However, comparative analyses of various metal-loaded alumina catalysts for the reductive catalytic fractionation process are rare. Moreover, most research relies on high-pressure hydrogen, which poses safety risks, increases costs, and limits scalability, highlighting the need for further optimization [10].

Reductive catalytic fractionation oil is an attractive lignin-derived feedstock, owing to its high content of monomers, good solubility and stability. Commercial products can be obtained through extraction and purification, such as phenolic compounds, which are recognized as natural antioxidants [11]. Besides, the integration of hydrodeoxygenation technologies can further produce arenes and cycloalkanes. Kordouli and colleagues used Rh, Ni, and Mo-Ni catalysts supported on carbon to catalyze the hydrodeoxygenation of phenol to cyclohexane. However, the reaction required a temperature of 310 °C and a hydrogen pressure of 3 MPa [12]. Fortunately, Li et al. recently demonstrated a high conversion of dihydroeugenol to C9 hydrocarbons using Ru/C and Nb_2O_5 co-catalysis. The reaction, conducted at 250 °C under an initial H_2 pressure of 6 bar at room temperature, showcased the synergistic effect of metal and acidic sites in promoting deoxygenation [13]. The slight downside is the lack of experimental validation for the actual depolymerized bio-oils and the insufficient screening of solvents.

While numerous approaches have been proposed for lignin valorization, the fate of holocellulose as solid residue has rarely been explored. Typically, holocellulose is hydrolyzed and fermented to produce bioethanol [14]. However, without catalyst recovery, fermentation of solid residues may face significant challenges due to potential catalyst toxicity [15]. Integrating a tandem chemocatalytic approach is a promising option for enhancing downstream holocellulose upgrading. However, this transformation process is typically conducted with the assistance of expensive and toxic solvents [16]. Thermochemical processes offer viable solutions for converting waste into biofuels and biochemicals [17]. Notably, fast pyrolysis is a direct biomass liquefaction technology favored by researchers for its scalability, feedstock versatility, high energy efficiency, and strong environmental performance [18]. Additionally, its emerging potential for machine learning-based predictive modeling could further optimize processes and drive technological advancement [19]. An extensive literature review reveals that while cellulose pyrolysis has been thoroughly studied, research on the downstream pyrolytic conversion of solid residues from "lignin-first" biorefineries remains scarce. Hu et al. conducted preliminary research on the pyrolysis of holocellulose derived from upstream reductive catalytic fractionation processes, revealing high char yields and low bio-oil yields, which were less than ideal [20]. There is an urgent need to strategically develop reaction systems that achieve convergence and balance between upstream fractionation and downstream upgrading. More importantly, a comprehensive system-level analysis that considers multiple factors, including carbon, energy, economy, and environment, is crucial for identifying potential challenges and opportunities for commercialization [21].

This study presents a novel strategy that eliminates the need for high-pressure hydrogen and complex chemical reagents (Fig. S1). Ni/Al_2O_3, Mo/Al_2O_3, and NiMo/Al_2O_3 catalysts were selected for H_2-free reductive catalytic fractionation, offering a rare comparative analysis to fill the research gap. The synergistic effects of different metals were explored through experimental analysis and catalyst characterization. Subsequently, concentrated aromatic bio-oils from the upstream process were converted into hydrocarbons via mild hydrodeoxygenation, while holocellulose-rich residues underwent catalytic pyrolysis to produce alternative fuels and furfural compounds, utilizing the same NiMo/Al_2O_3 catalyst as in the preceding step. Moreover, process modeling and evaluation of the entire system are conducted to assess carbon utilization efficiency, energy recovery, potential environmental impacts, and cost-effectiveness. This work aims to enhance the potential of this novel strategy, identify setbacks, and drive advancements in energy and chemical engineering.

2. Materials and methods

2.1. Materials for the experimental study

Poplar powder, provided by Qilu University of Technology, was used as the biomass feedstock. The moisture content of raw poplar materials is about 8.1 %. The Ni/Al_2O_3, Mo/Al_2O_3, and NiMo/Al_2O_3 catalysts investigated in this study were prepared by the wet impregnation method, using $Ni(NO_3)_2 \bullet 6H_2O$ and $(NH_4)_6Mo_7O_{24} \bullet 4H_2O$ as precursors [22]. $NbCl_5$ and $RuCl_3$ were purchased from Shanghai Aladdin Biochemical Technology Co., Ltd., China. Nb_2O_5 was synthesized using the sol-gel method [23]. Typically, $NbCl_5$ (20 mmol) was dissolved in ethanol (20 mL) under stirring and then added dropwise to a CTAB solution (1 g in 15 mL of distilled water). After further stirring, an HCl solution (20 mL, pH ~1) was introduced, and the mixture was stirred again. The solution was aged at 160 °C for 24 h in a Teflon-lined autoclave, after which the solid was separated, washed, and dried at 60 °C overnight. After grinding, the solid was calcined at 450 °C for 6 h. Subsequently, a 2 wt% Ru/Nb_2O_5 catalyst was prepared using the equal-volume impregnation method. All catalysts were thermally reduced in a 10 % H_2/Ar flow, then passivation was performed at room temperature with 100 mL/min of 0.5 % O_2/N_2 for 30 min. Acetone and hexane were purchased from Sigma-Aldrich, while methanol, ethanol, and other chemicals were obtained from Sinopharm Chemical Reagent Co., Ltd. All commercial reagents were used as received, without further purification.

2.2. Reductive catalytic fractionation

Reductive catalytic fractionation was carried out in a 50 mL stainless steel batch reactor supplied by LABE Instrument Co., Ltd., equipped with a magnetic stirrer. Typically, poplar powder (1.0 g), metal-loaded alumina catalyst (0.1 g), and 20 mL methanol were placed in the reactor. After the autoclave was sealed, it was flushed with nitrogen 3 times and pressurized with nitrogen (0–4 MPa). Then reactants were stirred at 600 rpm and heated to 200–275 °C at a rate of 10 °C/min. Holding at this temperature for 3 h before quench cooling. The liquid fraction was filtered from solid residues, with a small amount of extra methanol used to wash the residues. Thereafter, the pooled liquid mixture was concentrated using a vacuum rotary evaporator (200 mbar, 50 °C) to obtain crude aromatic bio-oils.

Herein, the characterization of various metal-loaded alumina catalysts was also performed. Specifically, the X-ray diffractometer (XRD, Rigaku Ultimate IV) with a Cu Kα anode ($\lambda = 1.5418$ Å) was applied to obtain information about crystal structure of materials. X-ray photoelectron spectroscopy (XPS) using the Thermo Scientific K-Alpha instrument was employed to identify the chemical states of metals in various catalysts, with corresponding binding energies and associated chemical shifts collected. The Micromeritics ASAP 2460 equipment was employed to acquire N_2 adsorption-desorption isotherms, allowing for the determination of specific surface area, pore volume, pore size, etc. Ammonia temperature programmed desorption was performed to characterize the surface acidity of various catalysts.

2.3. Mild hydrodeoxygenation

Batch reactions were also conducted in the 50 mL autoclave reactor, heated to 250 °C using an insulated furnace. For all tests, 0.2 g of Ru/Nb_2O_5 catalyst was used each time to facilitate mild upgrading. The reaction substrate includes not only a mixture of model compounds but

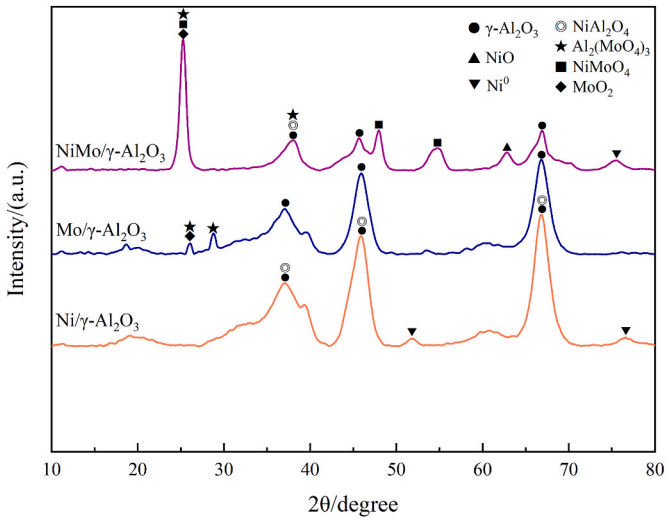

Fig. 1. XRD patterns of various metal-loaded alumina catalysts.

also actual concentrated reductive catalytic fractionation oil. The model compounds were selected based on typical aromatic monomers generated from H_2-free reductive catalytic fractionation, and detailed compositional information is provided in Table S1. Specifically, a 250 mL mixed solution was prepared in advance, with 16 mL used for each experiment. Hexane was used as the solvent due to its excellent performance reported in previous hydrodeoxygenation studies, particularly for its dual role in promoting hydrogen transfer and inhibiting coke formation [24]. Therefore, optimization of model compounds upgradation was performed in hexane with different hydrogen pressures and reaction times. Additionally, the hydrodeoxygenation of actual concentrated bio-oils (~0.4 g) was evaluated using various solvents (~16 mL), including acetone, water, methanol, and hexane. Furthermore, approximately 16 mL of hexane was used to extract concentrated aromatic bio-oils from the reductive catalytic fractionation of 2 g of poplar feedstock. The distribution of bio-oil components from hexane extraction can also be found in the Supplementary Material.

2.4. Analytics pyrolysis

After delignification pretreatment, separated solid residues (mixture of catalyst and remaining biomass) were dried at 75 °C overnight, exposed to ambient air. The samples were carefully weighed, ensuring that the remaining biomass weighed approximately 0.5 mg, and then placed in a micro crucible. Initially, analytics pyrolysis experiments were carried out on a set of micro-furnace pyrolyzer (EGA PY-3030D)-GC/MS (ISQ 7000) system to optimize pyrolysis temperature. Meanwhile, raw poplar as control group to display the influence of reductive catalytic fractionation treatment. Subsequently, effects of catalyst/reactant mass ratio (C/R: 0.2–2) were further investigated. Test was repeated for three times to obtain reliable results. All samples were grounded over 20 min before testing to assure that the mixture was homogeneous enough.

2.5. Products analysis

Qualitative analysis was performed using a GC-MS (8860-5977B, Agilent Technologies, USA), with helium as the carrier gas. Particularly, the autosampler aspirated a 1 μL volume of liquid sample into the GC column after reductive catalytic fractionation and hydrodeoxygenation experiments while reaction gas directly swept reaction products into the downstream GC during analytics pyrolysis. In the three types of experiments mentioned above, all ideal products were quantified using external standard methods. The following formulas were used to calculate the yield and selectivity of ideal products:

$$Mass\ yield\ (wt\%) = \frac{Weight\ of\ ideal\ products}{Weight\ of\ substrates} \times 100 \quad (1)$$

$$Selectivity\ (\%) = \frac{Peak\ area\ of\ ideal\ products}{Peak\ area\ of\ total\ identified\ products} \times 100 \quad (2)$$

$$Carbon\ yield\ (\%) = \frac{C-mol\ of\ ideal\ products}{C-mol\ of\ substrates} \times 100 \quad (3)$$

2.6. Process modeling and evaluation

Based on experimental data, the process model was simulated using Aspen Plus V10 software. Herein, the plant design with a poplar flow rate of 2000 dry metric tonne/day was consistent with previous publications, allowing for comparative analysis with other biomass valorization models [25,26]. The corresponding process flow sheet is shown in Fig. S2, and the assumptions for process modeling are detailed in the Supplementary Material. By analyzing material and energy flow data across the entire conversion process, a thorough assessment was conducted to identify key points of carbon and energy loss. Specifically, carbon accounting for poplar utilization was conducted on the basis of biomass conversion, with biogenic carbon flows quantified to identify the crucial carbon loss step [27,28]. To better understand the development of system energy utilization, several key evaluation indicators such as fuels yield, energy conversion rate, and energy efficiency were considered in the research. Relevant calculation equations can also be found in the Supplementary Material.

Besides, the potential cost and environmental impact of the proposed wood-based biorefinery were evaluated. Techno-economic analysis can provide insights into identifying the most impactful elements and enhancing economic feasibility. The "Nth-plant" assumption was adopted to avoid accounting for additional costs associated with "first of a kind" plants, such as special financing, equipment redundancies, large contingencies and longer start-up times. Detail economic assumptions are summarized in Table S2, and estimation methods have been documented in previous research [26]. Employing discounted cash flow method to calculate the minimum fuel selling price, which serves as an economic index to assess the pinch points of the proposed graded utilization system. Life cycle assessment is a tool used to evaluate and identify the most relevant environmental impacts and hotspots throughout the life cycle of a product or process. The functional unit applied is 1 MJ of biofuel at the biorefinery gate. All inputs and outputs from the biorefinery were assessed relative to the amount needed to produce 1 MJ of liquid fuel (Table S3). Originally, the cradle-to-gate life cycle assessment of the catalysts was conducted, and it was found that the catalysts contribute minimally to overall GHG emissions (<0.5 %), which is consistent with Tschulkow's observation [29]. This is attributed to the assumption that the $NiMo/Al_2O_3$ and Ru/Nb_2O_5 catalysts are replaced annually, which reduces the GHG emissions per unit produced. Therefore, additional key assumptions, including the potential for the buildings to be repurposed for other uses and the catalysts' relative stability throughout their life cycle, led to their exclusion from the assessment [30]. Seven impact categories were selected because they represent significant environmental issues in China, including Abiotic Depletion Potential (ADP), Acidification Potential (AP), Eutrophication Potential (EP), Global Warming Potential (GWP), Human Toxicity Potential (HTP), Ozone Depletion Potential (ODP), and Photochemical Ozone Creation Potential (POCP). Characterization and normalization were performed using standard procedures [27]. In this work, the products include biofuels, chemicals, and electricity, so commonly used economic and energy allocation approaches were considered [31]. For identifying key process parameters and their influence on the environmental impacts within the process, possible changes have been proposed in the main biorefinery process.

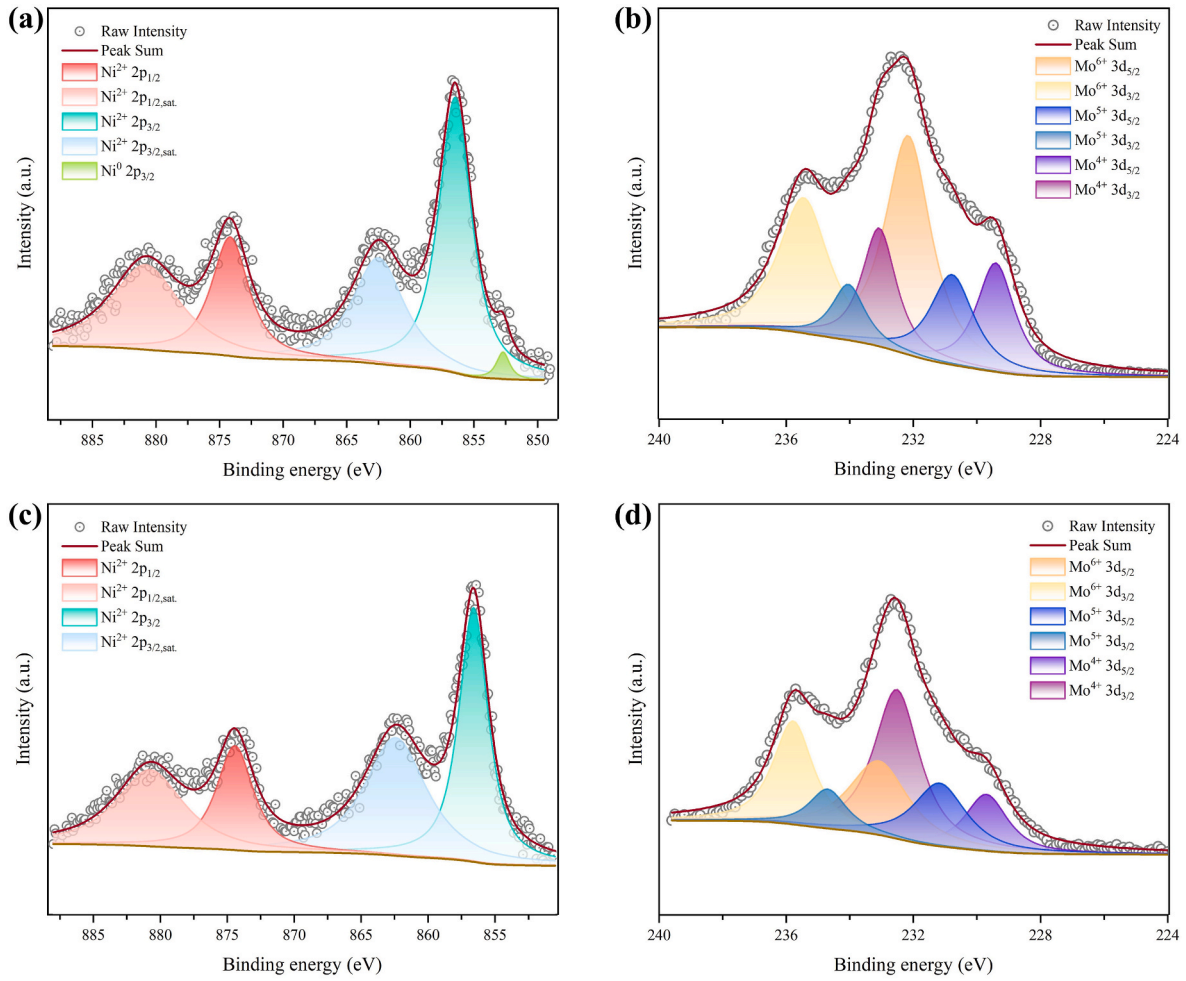

Fig. 2. XPS spectra of (a) Ni/Al_2O_3 for Ni 2p; (b) Mo/Al_2O_3 for Mo 3d; $NiMo/Al_2O_3$ for (c) Ni 2p and (d) Mo 3d.

3. Results and discussion

3.1. Catalysts characterization and reaction optimization for reductive catalytic fractionation

Fig. 1 displays XRD spectras recorded in the 2θ range of 10–80°. The diffraction peaks corresponding to Al_2O_3 species were observed at 2θ = 37°, 46°, and 67° in all samples, and their properties are well-documented [32,33]. Due to reflection overlap between phases, distinguishing $NiAl_2O_4$ from Al_2O_3 on the diffractogram is unclear in Ni/Al_2O_3. Since samples underwent thermal reduction treatment prior to testing, diffraction peaks from Ni^0 were detected while NiO species were not observed. It should be noted that the observed intensity was not significant, which indicates that the loading is relatively uniform and the metal is well dispersed [34]. For Mo/Al_2O_3 catalyst, $Al_2(MoO_4)_3$ species were observed near 26° and 29°, in addition to the diffraction peaks of MoO_2 at 26°. Diffraction peaks of $Al_2(MoO_4)_3$, $NiMoO_4$, $NiAl_2O_4$, MoO_2, NiO, and Ni^0 were all detected in $NiMo/Al_2O_3$. The coexistence of polycrystalline phases and the notably intense Mo peaks indicate the potential of bimetallic catalysts for higher activity during catalytic reactions. Interestingly, it comes at the expense of a decrease in the peak of the Al_2O_3 carrier, which was covered so that the corresponding diffraction peaks were diluted [33].

XPS analysis provides valuable insights into the chemical states of nickel and molybdenum in the catalysts (Fig. 2). The Ni 2p 1/2 peak appear at 875.8 eV and the corresponding satellite peak caused by multi-electron excitations of Ni^{2+} is observed at 880.5 eV. For Ni 2p 3/2, the peak centered at 854.2 eV corresponds to Ni^{2+} within the NiO structure, while peaks around 856.7 eV and 857 eV correspond to Ni^{2+} in $NiMoO_4$ and $NiAl_2O_4$, respectively. Additionally, the peak near 862.2 eV is assigned to the vibrational satellite structure of Ni 2p 3/2. No peaks definitively associated with NiO were identified in the Ni/Al_2O_3 and $NiMo/Al_2O_3$ catalysts used in this study, indicating that the majority of nickel atoms react with alumina and/or molybdenum oxide to produce $NiAl_2O_4$ and/or $NiMoO_4$ [35]. Notably, a small peak corresponding to the 2p 3/2 binding energy shift of Ni metal was also observed at 852.6 eV in the Ni/Al_2O_3 catalyst, aligning with the XRD characterization results. In the analysis of the Mo 3d spectra, peaks around 229.6 eV and 232.9 eV can be attributed to the 3d 5/2 and 3d 3/2 states of the Mo^{4+} species, respectively. Peaks centered at 231.5 eV and 234.7 eV correspond to 3d 5/2 and 3d 3/2 states of the Mo^{5+} species, respectively. Peaks around 233.0 eV and 236.2 eV can be assigned to the 3d 5/2 and 3d 3/2 states of the Mo^{6+} species, respectively. Typically, Mo^{4+} species indicate the formation of MoO_2, Mo^{5+} species correspond to partially reduced Mo oxides, and Mo^{6+} species signify MoO_3. Quantitative analysis revealed that the peak area ratios for Mo^{4+}, Mo^{5+}, and Mo^{6+} species in Mo/Al_2O_3 and $NiMo/Al_2O_3$ catalysts were 26 %:19 %:55 % and 41 %:21 %:38 %, respectively. A significant increase in the relative content of low-valent-state Mo in NiMo bimetallic catalysts is likely due to the presence of nickel, which facilitates the reduction of MoO_3. It is noteworthy that the formation of oxygen vacancies in the catalyst tends to promote the adsorption and activation of oxygenates, thereby facilitating the production of additional phenolic monomers [36].

According to the IUPAC classification, the isotherms for all three catalysts exhibit type IVa characteristics, indicating mesoporous material properties (Fig. 3). It was also verified by the results of pore size

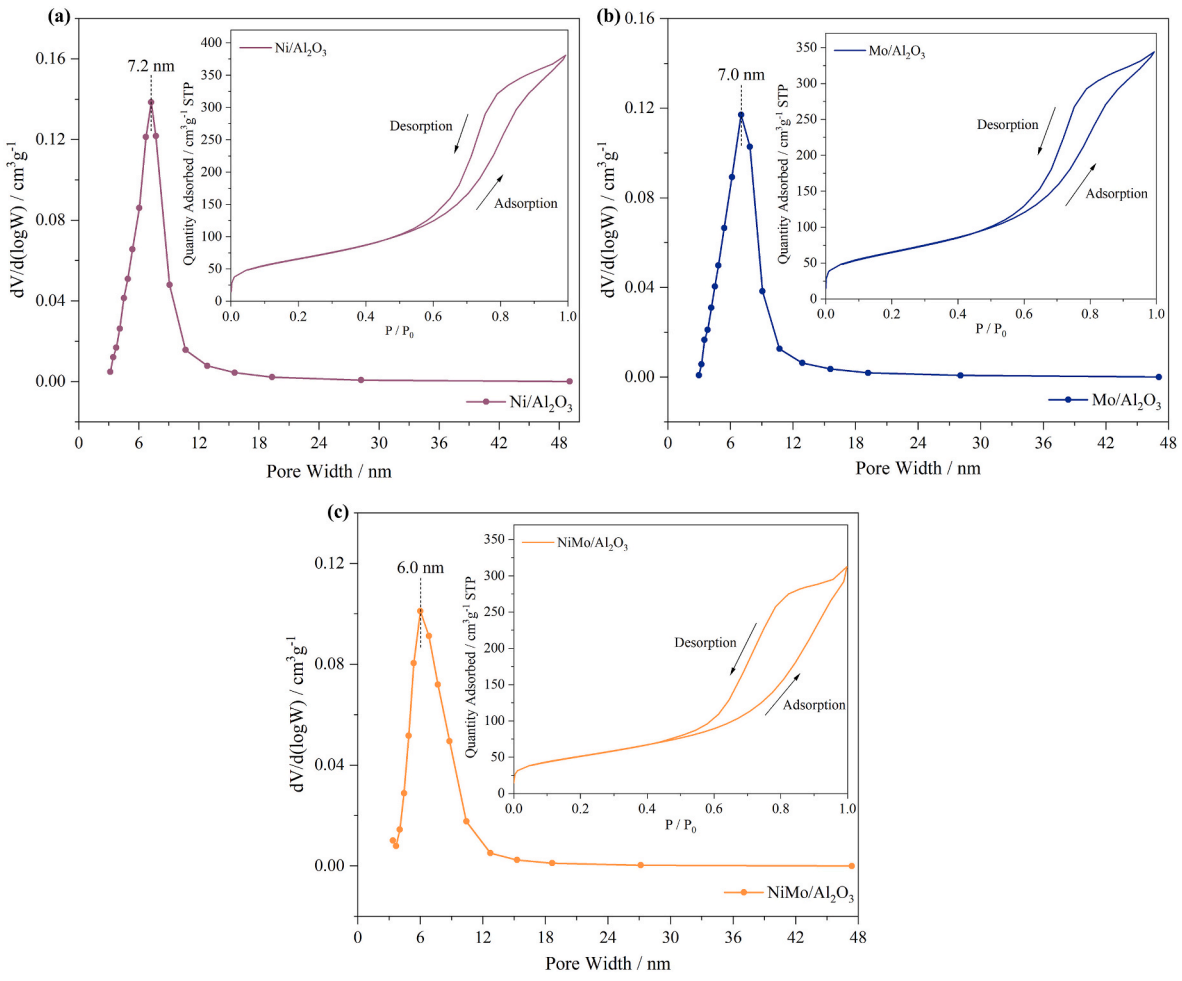

Fig. 3. Nitrogen adsorption-desorption curve (inside) and pore size distribution (outside) of (a) Ni/Al_2O_3; (b) Mo/Al_2O_3; (c) $NiMo/Al_2O_3$.

Table 1
Pore structure and acid properties of various metal-loaded alumina catalysts.

Samples	S_{BET}	V_{Total}	Average pore size	Total acid (Weak: Medium: Strong)
	m^2/g	cm^3/g	nm	μmol/g
Ni/Al_2O_3	230	0.6	7.5	294 (74 %: 16 %: 10 %)
Mo/Al_2O_3	230	0.5	7.3	513 (100 %: 0 %: 0 %)
$NiMo/Al_2O_3$	283	0.5	6.5	267 (45 %: 0 %: 55 %)

distribution, which revealed prominent mesoporous peaks. More specifically, Ni/Al_2O_3 and Mo/Al_2O_3 catalysts exhibit H4-like hysteresis loop isotherms without any discernible saturation adsorption plateau, which is often attributed to slit-shaped pores. However, $NiMo/Al_2O_3$ samples tend to exhibit H2-type hysteresis loop isotherms, distinguished by a saturated adsorption plateau and larger hysteresis loops, suggesting a more uniform pore size distribution. Notably, the $NiMo/Al_2O_3$ catalyst, with smaller average pore size, larger specific surface area, and more uniform pore distribution, is expected to offer more available active sites (Table 1). Moreover, it should be noted that different metal species on Al_2O_3 may change the distribution of acidic sites in the catalyst [37]. Ni/Al_2O_3 catalyst and Mo/Al_2O_3 catalyst exhibited larger total acid amounts and more weak acid sites. By contrast, the total acid amount of the $NiMo/Al_2O_3$ catalyst decreased to 266.6 μmol/g, while there was a significant increase in the proportion of strong acid sites and a decrease in the proportion of weak acid sites within this catalyst. Bimetallic doping is an effective strategy to optimize the acidic site distribution, which may lead to the creation of new active sites and thus enhance the catalytic activity.

Comprehensive studies on reductive catalytic fractionation were conducted with the comparison of various catalysts and reaction parameters. As illustrated in Fig. 4a, the highest yield of lignin-derived aromatic monomers was achieved with $NiMo/Al_2O_3$, and the catalytic performance decreased in the following order: $NiMo/Al_2O_3$ > Ni/Al_2O_3 > Ni/Al_2O_3&Mo/Al_2O_3 > Mo/Al_2O_3. Metal-loaded alumina catalysts have been utilized for macromolecular deconstruction, not only in biomass conversion but also in lignin valorization [38–40]. Achieving high aromatic monomer yields relies on effectively depolymerizing lignin. Given that C-C interunit linkages in lignin can't be cleaved under the applied reaction conditions, lignin depolymerization is primarily driven by ether bond cleavage. To clarify the specific roles of the metal catalyst and solvent, each individual step has been investigated using 2D HSQC NMR and GPC techniques. As reported by Van den Bosch et al., methanol serves both as a solvent, promoting the solvolytic cleavage of β-O-4 bonds, and as a hydrogen donor, aiding in the reduction of unsaturated compounds. The $Ni\text{-}Al_2O_3$ catalyst primarily functions to

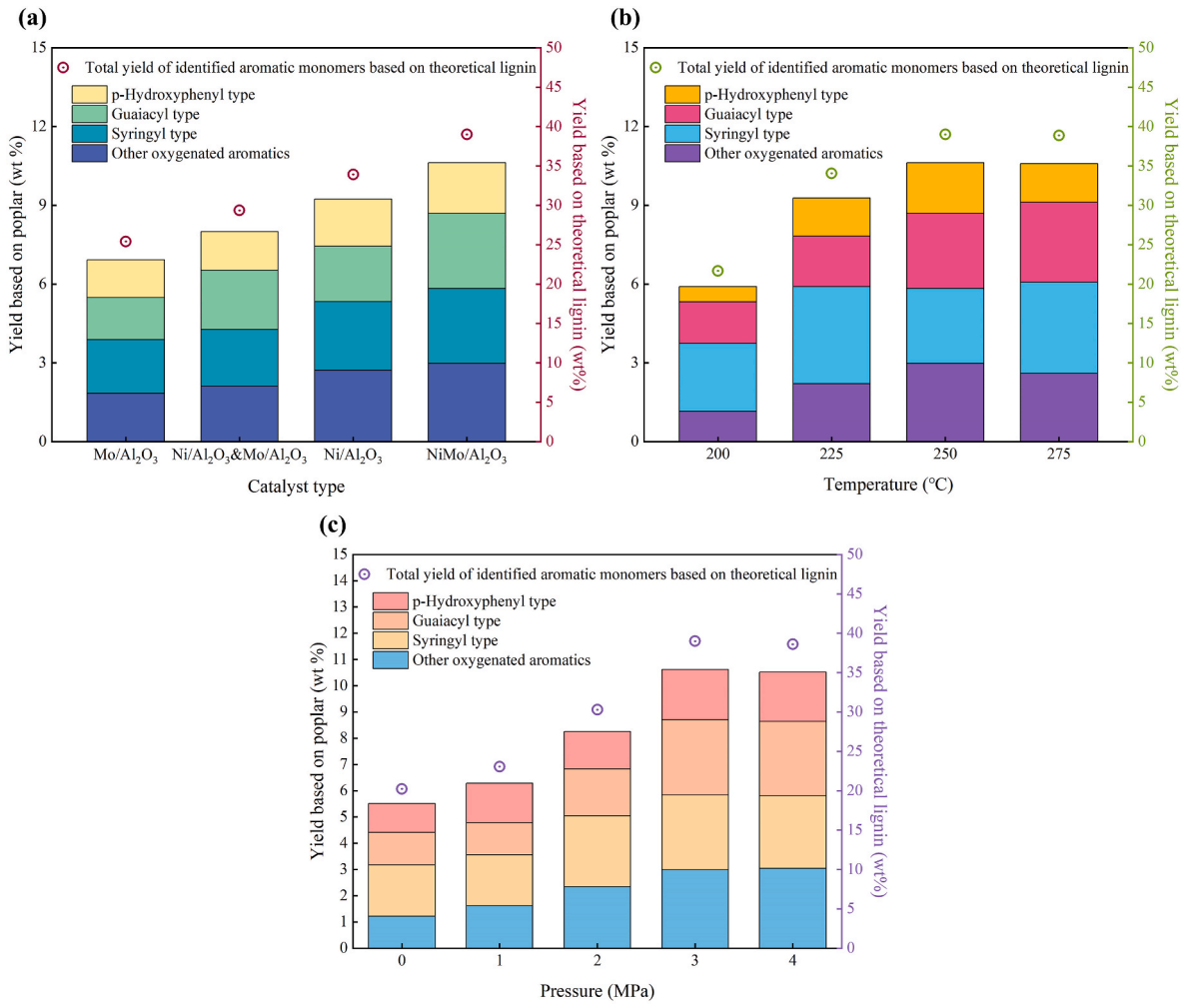

Fig. 4. Reaction optimization for reductive catalytic fractionation with (a) various metal-loaded alumina catalysts at 250 °C and 3 MPa nitrogen; (b) different temperatures using the NiMo/Al_2O_3 catalyst at 3 MPa nitrogen; and (c) different pressures at 250 °C using the NiMo/Al_2O_3 catalyst.

hydrogenate the unsaturated side chains of intermediates, thereby stabilizing the system and preventing rapid repolymerization [9]. As is well known, bimetallic NiMo catalysts exhibit superior catalytic hydrogenation activity compared to monometallic catalysts, which may explain the high aromatic monomer yield obtained with NiMo/Al_2O_3 [33,41]. However, a simple physical mixture of Ni/Al_2O_3 and Mo/Al_2O_3 catalysts in a 1:1 mass ratio did not show any advantages. This highlights the importance of the synergistic interaction between the Ni and Mo species, which enhances the catalyst's performance. Moreover, acid sites can adsorb C-O bond of lignin due to its polar trait and readily available basic oxygen electronic doublet [42]. The higher concentration of strong acid sites in the NiMo/Al_2O_3 catalyst may contribute to the increased yield of target products, as studies have shown that abundant strong acid sites facilitate lignin depolymerization [43]. Additionally, it predominantly generates phenolic monomers with allyl groups, which enhance the dehydration of the propanol side chain due to the inherent acidity of the alumina support [44]. Fig. 4b illustrates the effect of reaction temperature on reductive catalytic fractionation over NiMo/Al_2O_3 catalyst within the temperature range of 200–275 °C. Based on the total lignin content in poplar, the mass yield of aromatic monomers was 21.68 wt% at 200 °C. It then increased gradually, reaching a maximum of 39 wt% at 250 °C. However, increasing the temperature to 275 °C did not result in a further enhancement of the monomer yield, likely due to the high temperatures inducing repolymerization reactions [45]. The influence of nitrogen pressure on yield and product distribution was further examined, with the results presented in Fig. 4c. Increasing the nitrogen pressure led to the improvement of monophenols, as seen in the case of 0 MPa, 1 MPa, 2 MPa and 3 MPa, 20.2 wt%, 23.1 wt%, 30.3 wt% and 39.0 wt% yields of total aromatic monomers were generated, respectively. Interestingly, a pressure of 3 MPa nitrogen was sufficient to reach the yield plateau by comparison with 4 MPa nitrogen (38.6 wt%). It should be noticed that can be seen that aromatic monomers derived from H_2-free reductive catalytic fractionation retain a diverse array of functional groups, including phenolic hydroxyl, methoxy, ester, aldehyde, and others (Fig. S3). This contrasts with the findings from earlier studies, which observed deeper defunctionalization to form relatively simpler products under a hydrogen atmosphere. Lignin-derived compounds, such as guaiacyl and syringyl-based monomers, as well as polyphenols, have been shown to effectively scavenge a wide range of free radicals. These compounds could serve as valuable antioxidant additives for biodiesel, enhancing its performance and improving system efficiency [46]. Notably, the selectivity for these high-value additives reached up to 60 % under the optimal operating conditions. Lignin-derived units act as antioxidants primarily because of the presence of phenolic hydroxyl groups, which interrupt the oxidation propagation reaction by donating hydrogen. It has been reported that phenolic compounds with a higher content of phenolic-hydroxyl groups, fewer aliphatic-hydroxyl groups, lower molecular weight, as well as narrower polydispersity generally exhibit enhanced antioxidant ability [47]. Therefore, inducing the hydrolysis of aliphatic-hydroxyl groups, such as the methoxy side chain on the benzene ring, for targeted conversion to phenolic-hydroxyl groups is expected to further enhance

Table 2
Performance with different reaction conditions.

Entry	Hydrogen pressure	Reaction time	Hydrocarbon yield (C-mol)	Product distribution (%)		
				Arene	Cycloalkane	Oxygenate
1	1 MPa	2 h	50.9 %	32.6 %	23.9 %	43.5 %
2	1 MPa	4 h	61.2 %	42.2 %	25.8 %	32.0 %
3	1 MPa	8 h	75.9 %	60.7 %	27.5 %	11.8 %
4	2 MPa	2 h	64.2 %	12.1 %	86.6 %	1.3 %
5	2 MPa	4 h	65.5 %	1.1 %	98.8 %	0.1 %
6	2 MPa	8 h	73.0 %	0.3 %	99.7 %	–
7	3 MPa	2 h	67.8 %	5.5 %	90.1 %	4.4 %
8	3 MPa	4 h	71.8 %	0.8 %	99.2 %	–
9	3 MPa	8 h	73.4 %	0.3 %	99.7 %	–

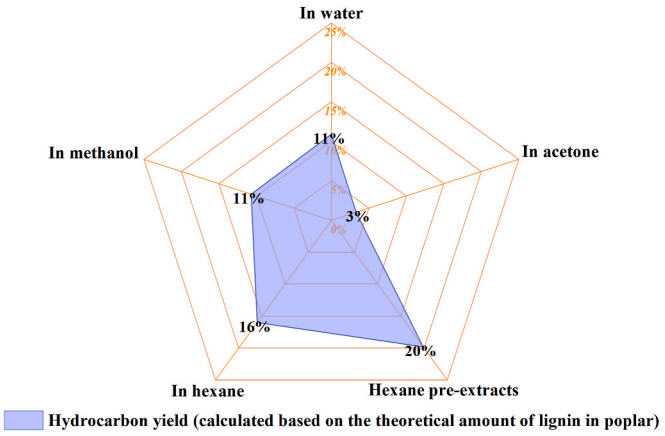

Fig. 5. Screening of solvents for hydrodeoxygenation of concentrated reductive catalytic fractionation oil.

antioxidant properties of lignin-depolymerized oils.

3.2. Mild hydrodeoxygenation of lignin derivatives

Reductive catalytic fractionation oil is rich in aromatic monomers, but their diverse chemical structures limit direct commercial application. Catalytic hydrodeoxygenation is an effective technology for consolidating lignin derivatives into a more refined and focused product range. Herein, initial screening was done to identify optimal reaction conditions by using a mixture of model compounds. As shown in Table 2, the conversion to fully deoxygenated products increases considerably with higher hydrogen pressure. It should be noted that under conditions of relatively low hydrogen pressure and short reaction times, oxygenates, including unreacted substrates (e.g., methyl benzoate, phenol, dihydroeugenol, methyl anisate, dimethyl terephthalate), and reaction intermediates (e.g., anisole, methyl phenol, 2,6-dimethylphenol, 4-propylphenol, 1,2-dimethoxy-4-propylbenzene, 1-methoxy-4-methylbenzene, etc.), still represent a significant proportion of the product distribution. When the hydrogen pressure exceeded 2 MPa and the reaction time surpassed 4 h, oxygenated compounds became almost undetectable in the products (<0.1 %). Meanwhile, the mass yield of hydrocarbon products and the corresponding C-mol yield remained above 50.7 % and 65.5 %, respectively. As hydrogen pressure increased, not only substrate deoxygenation but also aromatic ring hydrogenation became more pronounced. This is evidenced by the identification of intermediates such as 2-propylcyclohexanol and methyl cyclohexanecarboxylate under high hydrogen pressures and relatively short reaction times. However, the hydrogenation of aromatic rings, which was not the intended outcome, potentially leads to excessive hydrogen consumption. Remarkably, high selectivity for arenes was achieved at just 1 MPa of hydrogen pressure. Extending the reaction time further improved substrate conversion, especially at this low pressure. When the reaction time was extended from 2 h to 4 h and 8 h, the hydrocarbons yield (C-mol) increased by around 20 % and 49 %, respectively. Therefore, a moderate reduction in hydrogen pressure, coupled with an extension of the reaction time, may offer a more effective strategy for selectively producing aromatic hydrocarbon compounds. At a hydrogen pressure of 1 MPa and a reaction time of 8 h, the yield of hydrocarbons was 56.3 %, reaching a peak C-mol yield of 75.9 %. The primary products include cyclohexane, methylcyclohexane, benzene, toluene, p-xylene, propylcyclohexane, propylbenzene, and 1-methyl-4-propylbenzene, among others. Notably, arenes accounted for up to 69 % of the total hydrocarbon yield. Interestingly, during this reaction, the propyl side chain directly attached to the benzene ring was also altered, which differs slightly from the results observed under the Ru/C and Nb_2O_5 physical mixture catalytic system [13]. Dong et al. investigated the mechanisms using DFT calculations and confirmed that the NbO_x-supported catalyst shows significantly stronger substrate adsorption compared to other catalysts, which promotes the activation of C-C bonds and leads to efficient and selective cleavage of C-C linkages [48].

Subsequently, more experimental work was conducted to upgrade actual concentrated reductive catalytic fractionation oil. It's widely recognized that solvents significantly influence the catalytic performance in biomass upgrading. Therefore, the experimental effects in various solvents were compared in this study, with the results presented in Fig. 5. The highest yields of hydrocarbon products were achieved using hexane as the reaction medium, followed by water and methanol, while the lowest yields were obtained with acetone as the solvent. As reported in the literature, the use of n-hexane as a solvent may enhance hydrogen transfer and reduce the concentration of coke precursors, among other benefits. This contributes to sustained catalytic performance over a long period of time, facilitating increased hydrocarbon production [24]. Interestingly, when acetone served as the reaction medium, an increase in coupling products was observed. This indicates that the reaction system may foster competing reactions, like hydroxyl aldehyde condensation, which markedly impairs the catalyst's hydrodeoxygenation activity on lignin-derived compounds. Notably, under the optimal upgrading solvent (hexane), the yield of hydrocarbon products reached 16 wt% based on the theoretical lignin content in poplar. However, a portion of oxygenated compounds (~17.6 %) could still be detected after upgrading, which is noticeably higher than the 11.8 % observed in the corresponding model compound experiments under similar conditions. It is hypothesized that lignin-derived dimers and oligomers may be toxic to the catalyst's activity. This was evident after the hydrodeoxygenation of the actual depolymerized bio-oil, where the catalyst was found to be tightly adhered to the bottom of the vessel, showing a tendency to agglomerate and form coke. It has been reported that n-hexane allows for the cost-efficient extraction of aromatic monomers from lignin oil [49]. Thus, hexane pre-extracts of the actual oil were further explored to enhance substrate conversion and prevent catalyst deactivation. It was found that this approach further increased the hydrocarbon product yield to 20 wt% based on the theoretical lignin content in poplar. The used catalysts were easily collected and showed minimal deterioration, which indicates that the

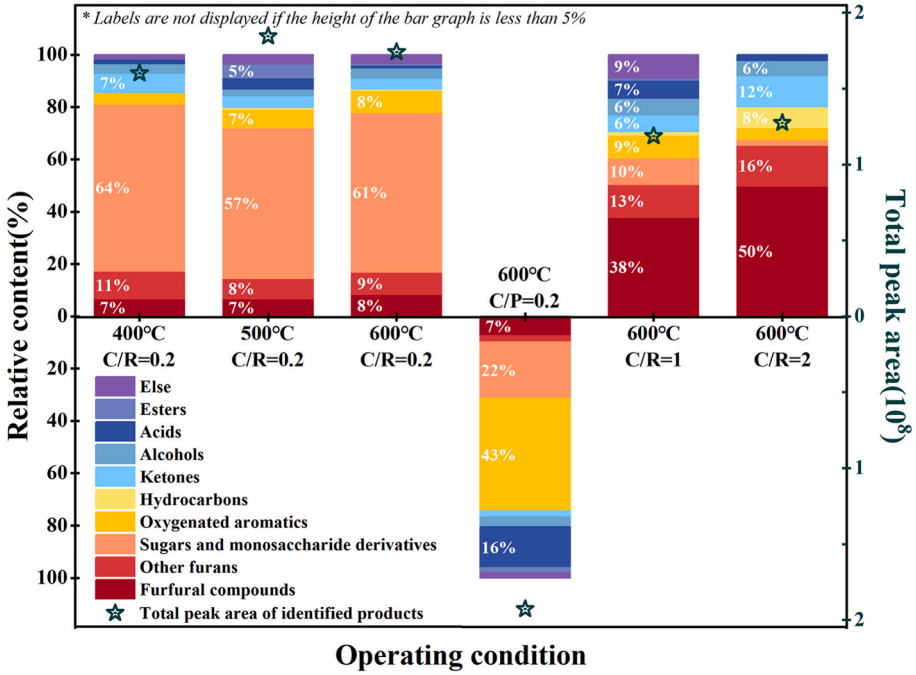

Fig. 6. Analytics pyrolysis of holocellulose-rich residues with different operating conditions.

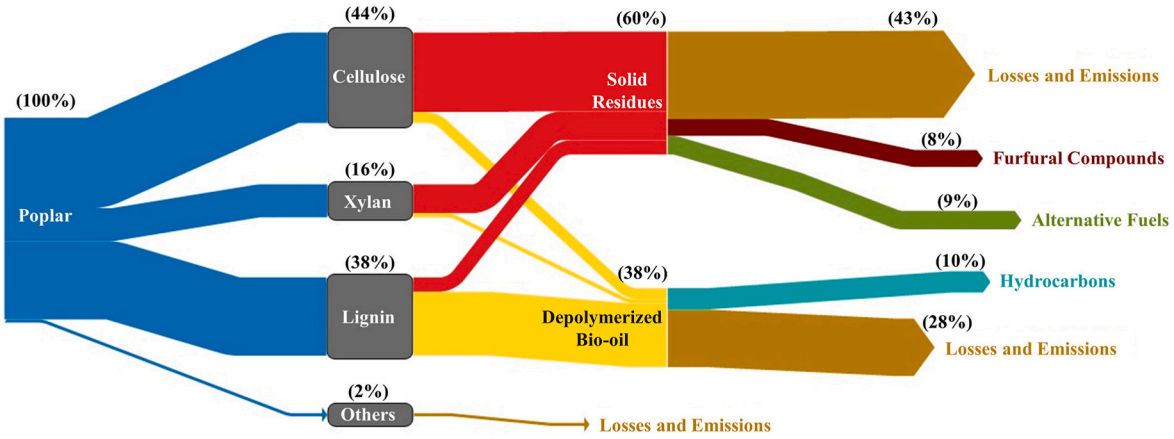

Fig. 7. Carbon footprint of the proposed system.

pre-purification of actual lignin-derived bio-oils could drop the difficulty of its further upgradation.

3.3. Py-GC/MS analysis of holocellulose-rich residues

Recent studies have indicated that the crystal structure and fiber morphology of the solid residue may be changed after delignification [50]. Herein, further experiments were carried out on holocellulose-rich residues to identify differences in pyrolysis characteristics (Fig. 6). Direct pyrolysis of the residue derived from NiMo/Al_2O_3-reductive catalytic fractionation revealed a dominance of primary sugar-derived compounds, including 3,4-Altrosan, sucrose, 1,6-Anhydro-α-d-galactofuranose, digitoxose, etc., which accounted for more than 50 % among all identified products. Notably, the highest amount of furfural compounds in the pyrolysis products was obtained at 600 °C. As depicted in the fourth column of Fig. 6, the reactant derived from reductive catalytic fractionation was replaced with raw poplar. With a consistent catalyst/reactant mass ratio, controlled experiments revealed that the selectivity for aromatic compounds in products from poplar pyrolysis was more than five times higher than in products from the pyrolysis of holocellulose-rich residues. This result confirms the successful delignification achieved through the pre-sequential reductive catalytic fractionation, as indicated by the main organic composition analysis shown in Table S4. More importantly, the yield of furfural compounds, other furans, ketones, sugars and monosaccharide derivatives generated from residues pyrolysis is obviously higher that of native poplar, which suggests that the presequential delignification treatment may facilitate the subsequent pyrolytic conversion of the (hemi)cellulosic fraction. The reason behind this is the facile decomposition of lignin-derived aryl ethers during pyrolysis, which generates free radicals that then undergo random polymerization, culminating in char formation. Cellulose-derived volatiles further interact with organic compounds on the surface of lignin-derived char through cross-polymerization, inducing the formation of carbonaceous deposits. No surprise, the thermochemical conversion of (hemi)cellulosic fractions would be limited [51].

The NiMo/Al_2O_3 catalyst has been shown to enhance biomass pyrolysis for liquid fuel production, primarily by facilitating hydrocracking

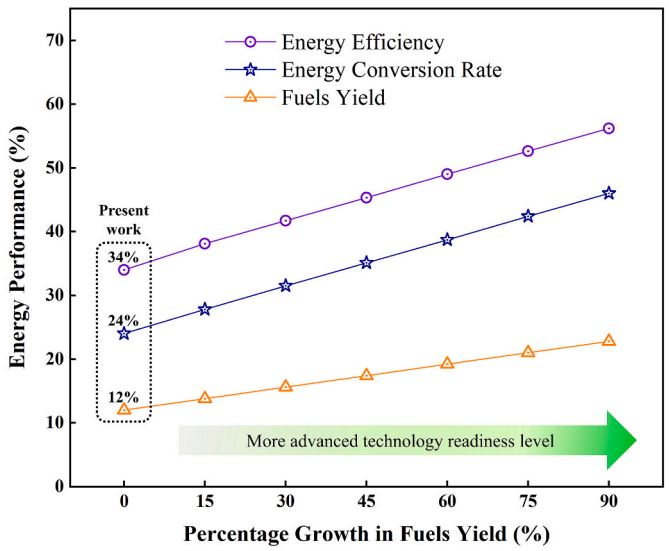

Fig. 8. Effect of enhanced fuel production on system energy performance.

and hydrodeoxygenation reactions, leading to the formation of aldehydes, furans, etc. [38]. In the present study, fresh catalyst was supplemented to ensure complete conversion of sugar-derived compounds, while used catalysts were easily collected from the coke tank for regeneration, eliminating concerns about recovery during pyrolysis. As the C/R ratio increased from 0.2 to 1 and then to 2, the selectivity towards furfural compounds rose from 8 % to 38 % and 50 %, respectively. Meanwhile, the presence of sugar-derived compounds decreased significantly, becoming nearly undetectable. At a C/R ratio of 2, the pyrolysis of holocellulose-rich residues predominantly yielded furfural compounds, alongside other furans, ketones, hydrocarbons, and a minor quantity of oxygenated aromatic compounds (Table S5). The standard compounds used for calibrating the products of interest are listed in the Supplementary Material, as shown in Table S6. Based on the bio-substrate content in residues derived from reductive catalytic fractionation, the sum total of mass yields of furfural, 3-furaldehyde, 5-methylfurfural, and 5-hydroxymethylfurfural products reached up to 10 wt%. Furfural compounds are recognized as one of the 12 high-value biomass-derived platform chemicals emphasized by the U.S. Department of Energy, drawing considerable attention from researchers owing to their remarkable versatility [52]. 9.4 wt% of (alkylated)furans, ketones, and hydrocarbons were also produced during residues pyrolysis. As reported by Hoang et al. and Jężak et al., (alkylated)furans such as methylfuran, with its gasoline-like properties, higher energy density than bioethanol, favorable octane/cetane numbers, and reduced water solubility, is a promising oxygenated biofuel that can be effectively blended into both gasoline and diesel engines to lower fossil fuel dependence and reduce soot formation [53,54]. It should be noted that ketones such as cyclopentanone, as oxygenated fuels, offer high knock resistance, improved efficiency, and lower emissions, making them a cost-effective and promising alternative for gasoline and diesel engines [55,56]. This indicates that the components generated during residue pyrolysis hold potential as alternative fuels for sustainable transportation, reducing dependence on fossil fuels.

3.4. *In-depth evaluation of the proposed system*

This innovative strategy can co-produce renewable fuels and high-value platform chemicals, such as furfural, with yields of up to 12.0 wt% and 6.5 wt%, respectively. Carbon accounting of poplar utilization was further conducted to quantify the extent of carbon usage within the system, as illustrated in Fig. 7. After the H_2-free reductive catalytic fractionation, approximately 10 % of the carbon from the feedstock is retained as hydrocarbons via hydrodeoxygenation of lignin derivatives. Meanwhile, during catalytic pyrolysis of holocellulose-rich residues, around 8 % and 9 % of the carbon from the feedstock are retained as furfural compounds and alternative fuels, respectively. Carbon loss mainly caused by the incomplete upgradation of bio-oil derived from reductive catalytic fractionation. While lignin monomers are efficiently converted, upgrading dimers and oligomers remains challenging. Although Román-Leshkov et al. achieved 87.5 % selectivity for aromatic hydrocarbons and 86 % theoretical carbon recovery from reductive catalytic fractionation oil using a two-stage catalytic process, the high-pressure and high-temperature conditions require further optimization and trade-off analysis [10]. Additionally, encouraging extensive research on the pyrolysis mechanism of dimer and trimer model compounds enables more efficient conversion of lignin dimers and oligomers [57]. More importantly, phenolic oligomers can also be used as

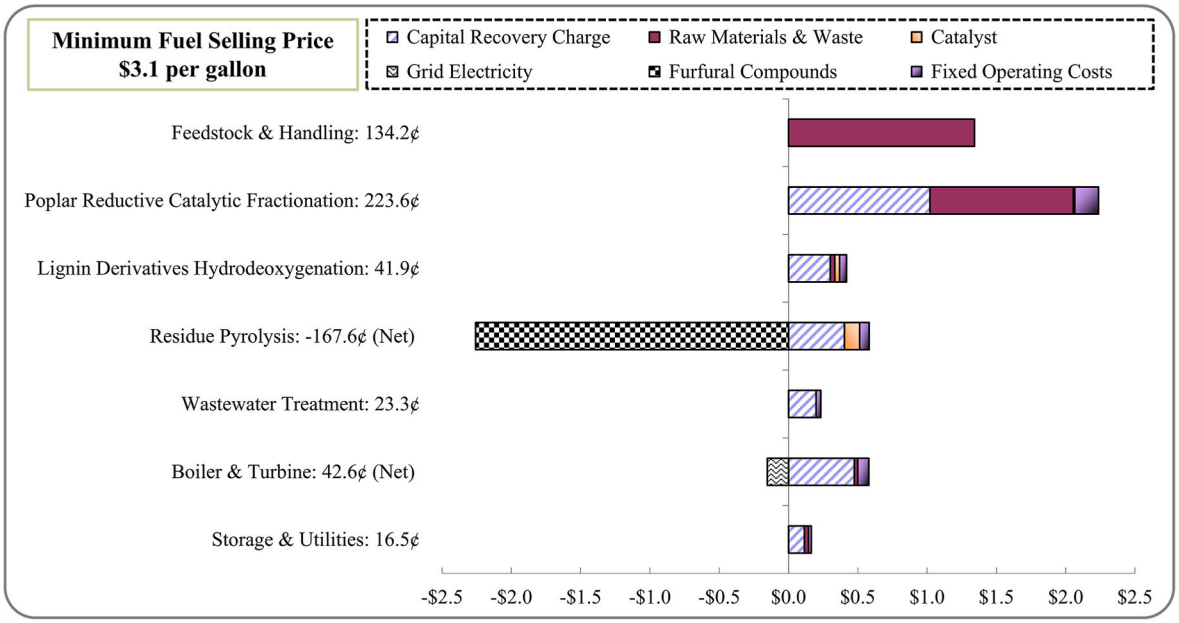

Fig. 9. Breakdown of the minimum fuel selling price.

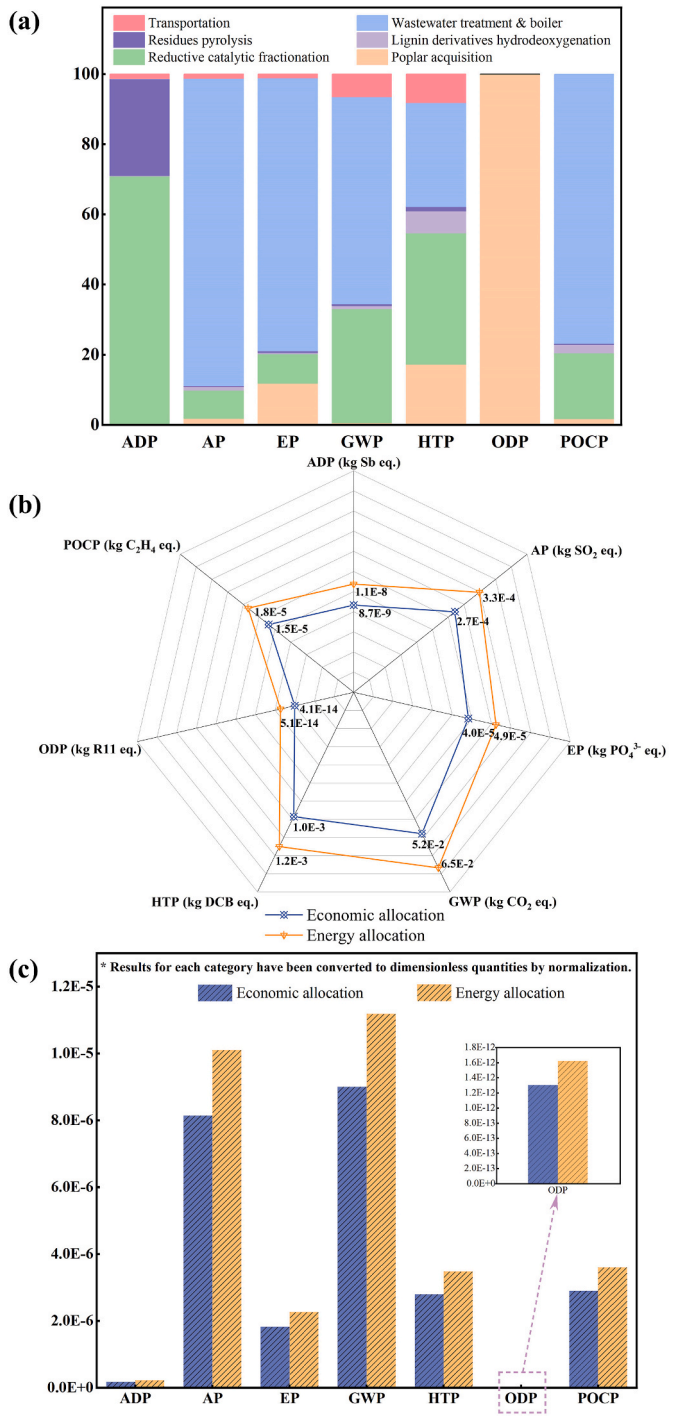

Fig. 10. Environmental impacts: (a) contribution analysis; (b) characterization values under different allocation methods; (c) normalization values under different allocation methods.

sustainable feedstock for resin production, such as ink and rigid polyurethane foam [49]. To improve the system's carbon efficiency, technological breakthroughs are required to valorize all components as efficiently as possible and prevent their disposal into the waste stream.

In this proposed biorefinery, fuels yield of 12 wt%, energy conversion rate of 24 %, and energy efficiency of 34 % are achieved. Notably, the efficient conversion of substrates to fuels, whether through the hydrodeoxygenation of lignin derivatives or the pyrolysis of residues, is crucial for determining the system's overall energy performance. Fuel products with higher calorific values contribute more significantly to the outcomes, suggesting that enhancing the conversion of lignin derivatives to hydrocarbons could be a more effective approach. Optimizing reaction conditions, such as pressure and heating rate, improving reactor design, and ensuring efficient collection of liquid products during pyrolysis are promising strategies for increasing fuel production, with further potential as advancements in technology readiness levels are anticipated [58,59]. Fig. 8 displays the impact of enhanced fuel production on system energy performance. It is evident that both the energy conversion rate and energy efficiency are strongly influenced by enhanced fuel production, which improved to 46 % and 56 %, respectively, when the yield of total fuel products increased to nearly 23 wt%. It is noteworthy that the energy efficiency indicator is influenced by a combination of fuel products and by-products such as furfural and electricity. In addition to enhancing fuel and chemical yields, optimizing system heat integration to convert excess heat into power by-products is also expected to significantly improve energy efficiency. Due to the high solvent loading and recovery requirements, hydrothermal liquefaction processes generally consume more energy. It is found that the parameter of solvent recovery rate has a significant impact on system energy accounting. Both methanol recovery rates of 96 % and 97 % ensure that the system can supply its own energy and produce electricity for sale, but the amount of electricity by-products decreases by approximately 49 % at 97 % compared to 96 %. With a 98 % methanol recovery rate, the system barely maintains heat balance but is not self-sufficient in power, requiring external power supply. In a previous study, under the ideal scenario of minimal organic solvent losses and a methanol recovery rate of 99.5 %, combustible waste combustion alone could not meet the energy requirements of the system. Consequently, an additional source of natural gas was introduced to supply heat and power to the system [25]. Herein, the unrecovered methanol can enter the anaerobic digestion unit as organic waste, generating biogas that supplies energy to the system through combustion, though this comes at the expense of organic solvents. Additionally, the solvent loading in the poplar reductive catalytic fractionation was set to 9 L/kg of dry biomass in the current simulation. The significant energy consumption caused by methanol recovery accounted for up to 70 % of the total system energy consumption. Fortunately, Beckham's team recently proposed a multi-pass flow-through reductive catalytic fractionation strategy, successfully reducing the solvent-to-biomass ratio to 1.9 L/kg. They found no significant degradation of lignin oil quality, effectively reducing the difficulty of solvent reusing and the associated energy demand [60]. In that case, when the solvent loading is reduced from 9 L/kg to 1.9 L/kg during the simulation, the energy efficiency of the system increases to 38.7 %, an improvement of nearly five percentage points.

Several economic metrics derived from techno-economic analysis were further evaluated, as illustrated in Table S7. The fixed capital investment and total capital investment are estimated at $588 million and $619 million, respectively, which is comparable to other wood biorefineries reported in the literature [26]. The plant's annual operating costs include $85 million in variable costs (feedstock, methanol, catalyst, hydrogen, etc.) and $14 million in fixed costs (salaries & labor burden, maintenance, insurance & taxes). A discounted cash flow model was constructed in Microsoft Excel, with iterative calculations used to determine the minimum fuel selling price that achieves a net present value of zero over a 30-year plant lifetime. The estimated minimum selling price of alternative fuels is approximately $3.1 per gallon, which is comparable to the reported range of $2.98 to $3.23 per gallon [61,62]. It also aligns closely with the average retail gasoline prices over the last five years, which is approximately $3.15 per gallon. Furthermore, the economic breakdown for respective process area regarding its contribution are summarized in Fig. 9. Among the different process areas, poplar reductive catalytic fractionation, boiler & turbine, and residue pyrolysis are the top three contributors to capital expenditures due to the high costs of pressure reactors, energy integration, and temperature-resistant reactors, respectively. Since equipment costs of reductive catalytic fractionation reactors constitutes a significant

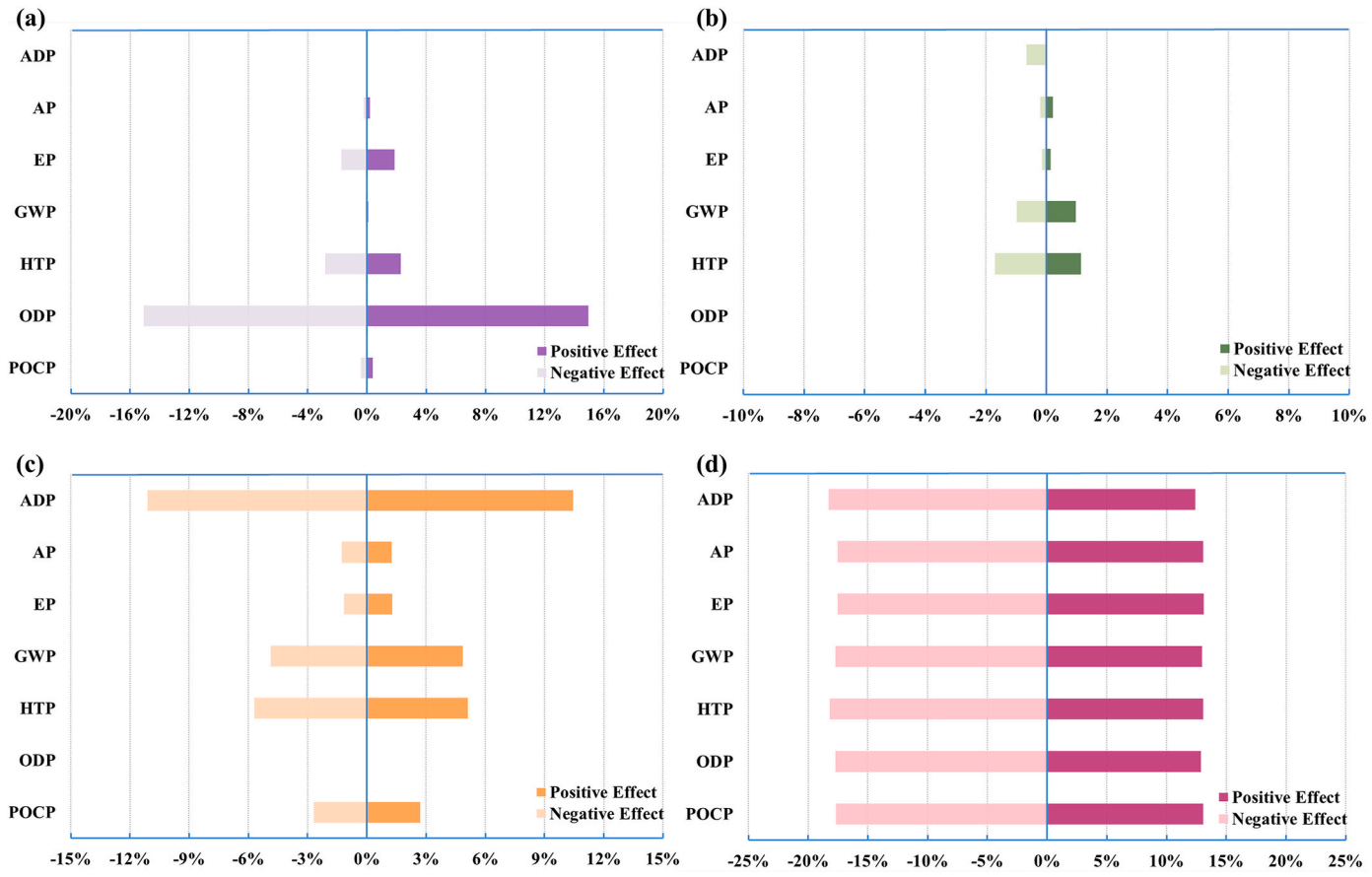

Fig. 11. Sensitivity analysis for life cycle assessment: (a) Fertilizer (±15 %); (b) Distance (±15 %); (c) Methanol loading (±15 %); (d) Ideal product yield (±15 %).

portion of the capital investment, altering variables related to the reactor's size and cost is expected to be effective in reducing overall expenses. For instance, reducing solvent loading can alter the system's heat integration and energy balance by decreasing the energy required for solvent recovery. Moreover, it will substantially decrease the necessary reactor volume, resulting in lower equipment costs. Sels' team successfully reduced the solvent-to-biomass ratio to 4 L/kg while achieving similar delignification efficiencies and lignin monomer yields [63]. In this case, the minimum fuel selling price would decrease by approximately 32 % to $2.1 per gallon. By then, the large-scale application of this novel strategy is expected to hit the gasoline industry. With distinct boiling point differences, furfural compounds can be efficiently separated from other components through fractional distillation, with the associated equipment and operating costs carefully considered (Table S7). It should be noted that revenues from furfural compound sales are substantial, offsetting costs and even providing an additional $1.68 per gallon. If the yield of furfural compounds can be further increased by 25 % through breakthroughs in pyrolysis technology, the minimum fuel selling price would be reduced by 17 %. Costs can also be offset to some extent via the generation of grid electricity. Additionally, the two largest cost components are biomass feedstock and methanol. In order to ensure stable sources of raw materials at low prices, it's also necessary to conduct supplier research and market analysis.

Fig. 10 presents the impact assessment results generated using GaBi software. To interpret the results and to identify the most significant contributors to various environmental impact categories, the entire system was divided into six sections: poplar acquisition, reductive catalytic fractionation, lignin derivatives hydrodeoxygenation, residues pyrolysis, wastewater treatment & boiler, and transportation. Fig. 10a clearly indicates that the system's environmental impacts primarily stem from reductive catalytic fractionation and wastewater treatment & boiler stages. The impacts from reductive catalytic fractionation are mainly due to the consumption of resources like methanol, while those from wastewater treatment & boiler are largely the result of emissions such as SO_2 and NO_x, as well as waste disposal. In addition, it is evident that the poplar acquisition section contributes significantly to ODP, primarily due to the application of N, P, and K fertilizers. The environmental impacts characterization values under different allocation methods can be found in Fig. 10b. Economic allocation seems to be the preferred approach when assessing co-products with different attributes. In this work, it can reduce all environmental impacts by approximately 20 % compared to energy allocation. To examine the significance of 7 environmental impacts categories, normalized results for each impact category were further considered, as shown in Fig. 10c. The comparative significance of each environmental impact category, ranked in order as GWP > AP > POCP > HTP > EP > ADP > ODP, remains consistent across both allocation methods. Notably, these results appear significantly different and much better than those from our previous research on biochemical technologies for poplar conversion, primarily due to the use of methanol instead of acids and complex chemicals during biomass fractionation [26].

Fig. 11 illustrates the sensitivity analysis results caused by ±15 % variations in selected parameters. The fertilizer employed in the agricultural process has a significant impact on the ODP, confirming that poplar acquisition serving as the primary contributor in this category. The environmental impacts associated with transportation distance appear to be relatively small. Methanol loading is a key variable, particularly exhibiting a significant fluctuation in ADP, with nearly a 10.5 % change. Meanwhile, a 15 % decrease in methanol loading leads to a reduction of the GWP value from 0.0524 to 0.0499 kg CO_2 eq./MJ, based on the economic allocation approach. The most notable influence on the environmental impacts is the ideal product yield. A 15 % increase

results in a 13 % variation in each category, while the adverse effect of a reduced yield is more pronounced, with a 15 % decrease leading to an 18 % variation in each category. Additionally, the variation in by-product credits, which can influence the allocation factor, was further examined in this study. Specifically, energy allocation considers only changes in by-product yields, while economic allocation also accounts for price fluctuations. When the input varies by 15 %, the rate of change for energy allocation was found to be 4.5 %, which is slightly lower than the 6.5 % observed for economic allocation. This work verified that biofuels have significant potential to reduce carbon emissions, as GHG emissions from fossil-based fuel production are approximately 0.0930 kg CO_2 eq./MJ. Last but not least, compared to other similar automotive biofuel production processes, such as pyrolysis (0.0648 kg CO_2 eq./MJ) and biochemical (0.0674 kg CO_2 eq./MJ) methods, the GWP value in the present research is approximately 19 % and 22 % lower, respectively [26,64]. Moreover, burden shifting to another environmental impact category (AP) is successfully avoided due to the efficient lime desulfurization and denitrification of tail gas, as well as the elimination of acid inputs.

4. Conclusion

This research presents a novel graded utilization strategy that integrates hydrothermal and pyrolysis technologies for woody biomass. It combines poplar reductive catalytic fractionation with lignin oil hydrodeoxygenation and residue catalytic pyrolysis, co-producing alternative fuels and furfural compounds, with mass yields of 12.0 % and 6.5 %, respectively. The synergistic effects of the bimetallic Ni-Mo catalyst were demonstrated by enhancing the activity of metal-loaded alumina catalysts, which led to increased yields of aromatic monomers. To further enhance carbon sequestration, it is crucial to explore novel catalysts and reaction pathways that maximize the efficient valorization of lignin dimers and oligomers. Additionally, increasing product yields and reducing solvent loading are expected to improve energy recovery. The estimated minimum fuel selling price closely aligns with the average retail gasoline prices over the past five years, but could potentially drop to $2.10 per gallon with the optimal solvent-to-biomass ratio. Notably, this strategy reduces carbon emissions by 44 % compared to fossil-based fuel production and by 20 % compared to other biofuel production methods. It also effectively avoids shifting the environmental burden to other impact categories. In summary, solvent-based processes require solvent recovery and recycling to be viable and effective. Multi-pass flow-through reductive catalytic fractionation offers a promising solution to address the challenge of high solvent usage. Additionally, membranes may provide a feasible alternative to distillation for recovering lignin oil and monomers. Further research should focus on optimizing reaction conditions and reactor design to enhance technical maturity and achieve efficient scaling, which will require ongoing collaborative efforts to unlock the full potential of these technologies and ensure their successful commercialization.

CRediT authorship contribution statement

Qian Qian: Writing – original draft, Visualization, Software, Formal analysis, Data curation, Conceptualization. **Zhongyang Luo:** Supervision, Project administration, Funding acquisition. **Feiting Miao:** Writing – review & editing, Methodology. **Caixia Song:** Writing – review & editing, Validation. **Jingkang Shi:** Methodology, Investigation. **Liwen Du:** Resources. **Qingguo Zhou:** Methodology. **Evgeny R. Naranov:** Methodology.

Declaration of competing interest

The authors declare that they have no known competing financial interests or personal relationships that could have appeared to influence the work reported in this paper.

Acknowledgement

This work was funded by the National Key Research and Development Program of China, No. 2023YFE0111600.

Appendix A. Supplementary data

Supplementary data to this article can be found online at https://doi.org/10.1016/j.energy.2025.135574.

Data availability

Data will be made available on request.

References

[1] Butera G, Gadsbøll RØ, Ravenni G, Ahrenfeldt J, Henriksen UB, Clausen LR. Thermodynamic analysis of methanol synthesis combining straw gasification and electrolysis via the low temperature circulating fluid bed gasifier and a char bed gas cleaning unit. Energy 2020;199:117405. https://doi.org/10.1016/j.energy.2020.117405.
[2] Ben Hnich K, Khila Z, Hajjaji N. Comprehensive study of three configurations coproducing synthetic fuels and electricity from palm residue via Fischer-Tropsch process. Energy 2020;205:118027. https://doi.org/10.1016/j.energy.2020.118027.
[3] Feng J, Hse C-y, Wang K, Yang Z, Jiang J, Xu J. Directional liquefaction of biomass for phenolic compounds and in situ hydrodeoxygenation upgrading of phenolics using bifunctional catalysts. Energy 2017;135:1–13. https://doi.org/10.1016/j.energy.2017.06.032.
[4] Ryu HW, Lee HW, Jae J, Park Y-K. Catalytic pyrolysis of lignin for the production of aromatic hydrocarbons: effect of magnesium oxide catalyst. Energy 2019;179:669–75. https://doi.org/10.1016/j.energy.2019.05.015.
[5] Yang D, Huang J, Hu Z, Qin S, Mu J, Wang F, et al. Catalytic pyrolysis of lignin to aromatic hydrocarbons over Nb/Al oxide catalyst. Energy 2024;302:131764. https://doi.org/10.1016/j.energy.2024.131764.
[6] Pang B, Sun Z, Wang L, Chen W-J, Sun Q, Cao X-F, et al. Improved value and carbon footprint by complete utilization of corncob lignocellulose. Chem Eng J 2021;419:129565. https://doi.org/10.1016/j.cej.2021.129565.
[7] Abu-Omar MM, Barta K, Beckham GT, Luterbacher JS, Ralph J, Rinaldi R, et al. Guidelines for performing lignin-first biorefining. Energy Environ Sci 2021;14(1):262–92. https://doi.org/10.1039/d0ee02870c.
[8] Luo H, Klein IM, Jiang Y, Zhu H, Liu B, Kenttämaa HI, et al. Total utilization of miscanthus biomass, lignin and carbohydrates, using earth abundant nickel catalyst. ACS Sustainable Chem Eng 2016;4(4):2316–22. https://doi.org/10.1021/acssuschemeng.5b01776.
[9] Van den Bosch S, Renders T, Kennis S, Koelewijn SF, Van den Bossche G, Vangeel T, et al. Integrating lignin valorization and bio-ethanol production: on the role of Ni-Al2O3catalyst pellets during lignin-first fractionation. Green Chem 2017;19(14):3313–26. https://doi.org/10.1039/c7gc01324h.
[10] Stone ML, Webber MS, Mounfield WP, Bell DC, Christensen E, Morais ARC, et al. Continuous hydrodeoxygenation of lignin to jet-range aromatic hydrocarbons. Joule 2022;6:2324–37. https://doi.org/10.1016/j.joule.2022.08.005.
[11] Zeb A. Concept, mechanism, and applications of phenolic antioxidants in foods. J Food Biochem 2020;44(9):1–22. https://doi.org/10.1111/jfbc.13394.
[12] Kordouli E, Kordulis C, Lycourghiotis A, Cole R, Vasudevan PT, Pawelec B, et al. HDO activity of carbon-supported Rh, Ni and Mo-Ni catalysts. Mol Catal 2017;441:209–20. https://doi.org/10.1016/j.mcat.2017.08.013.
[13] Li S, Liu B, Truong J, Luo Z, Ford PC, Abu-Omar MM. One-pot hydrodeoxygenation (HDO) of lignin monomers to C9 hydrocarbons co-catalysed by Ru/C and Nb2O5. Green Chem 2020;22(21):7406–16. https://doi.org/10.1039/d0gc01692f.
[14] Luo Z, Qian Q, Sun H, Wei Q, Zhou J, Wang K. Lignin-first biorefinery for converting lignocellulosic biomass into fuels and chemicals. Energies 2022;16:125. https://doi.org/10.3390/en16010125.
[15] Zhang J, Liu J, Kou L, Zhang X, Tan T. Bioethanol production from cellulose obtained from the catalytic hydro-deoxygenation (lignin-first refined to aviation fuel) of apple wood. Fuel 2019;250:245–53. https://doi.org/10.1016/j.fuel.2019.03.020.
[16] Guo T, Li X, Liu X, Guo Y, Wang Y. Catalytic transformation of lignocellulosic biomass into arenes, 5-hydroxymethylfurfural, and furfural. ChemSusChem 2018;11:2758–65. https://doi.org/10.1002/cssc.201800967.
[17] Fardi Z, Shahbeik H, Nosrati M, Motamedian E, Tabatabaei M, Aghbashlo M. Waste-to-energy: Co-pyrolysis of potato peel and macroalgae for biofuels and biochemicals. Environ Res 2024;242:117614. https://doi.org/10.1016/j.envres.2023.117614.
[18] Peters JF, Petrakopoulou F, Dufour J. Exergy analysis of synthetic biofuel production via fast pyrolysis and hydroupgrading. Energy 2015;79:325–36. https://doi.org/10.1016/j.energy.2014.11.019.
[19] Chen X, Shafizadeh A, Shahbeik H, Nadian MH, Golvirdizadeh M, Peng W, et al. Enhanced bio-oil production from biomass catalytic pyrolysis using machine learning. Renew Sustain Energy Rev 2025;209. https://doi.org/10.1016/j.rser.2024.115099.

[20] Hu Y, Oduro IN, Huang Y, Fang Y. Structural characterization and pyrolysis behavior of holocellulose obtained from lignin-first biorefinery. J Anal Appl Pyrolysis 2016;120:416–22. https://doi.org/10.1016/j.jaap.2016.06.012.
[21] Uekert T, Singh A, DesVeaux JS, Ghosh T, Bhatt A, Yadav G, et al. Technical, economic, and environmental comparison of closed-loop recycling technologies for common plastics. ACS Sustainable Chem Eng 2023;11(3):965–78. https://doi.org/10.1021/acssuschemeng.2c05497.
[22] Qian Q, Luo Z, Sun H, Wei Q, Shi J, Li S. Comparing physicochemical characteristics and depolymerization behaviors of lignins derived from different pretreatment processes. Fuel Process Technol 2023;250:107921. https://doi.org/10.1016/j.fuproc.2023.107921.
[23] Li S, Luo Z, Wang W, Sun H, Xie J, Liang X. Catalytic fast pyrolysis of enzymatic hydrolysis lignin over Lewis-acid catalyst niobium pentoxide and mechanism study. Bioresour Technol 2020;316:123853. https://doi.org/10.1016/j.biortech.2020.123853.
[24] Huang Y, Duan Y, Qiu S, Wang M, Ju C, Cao H, et al. Lignin-first biorefinery: a reusable catalyst for lignin depolymerization and application of lignin oil to jet fuel aromatics and polyurethane feedstock. Sustain Energy Fuels 2018;2(3):637–47. https://doi.org/10.1039/c7se00535k.
[25] Bartling A, Stone ML, Hanes RJ, Bhatt A, Zhang Y, Biddy MJ, et al. Techno-economic analysis and life cycle assessment of a biorefinery utilizing reductive catalytic fractionation. Energy Environ Sci 2021;14:4147–68. https://doi.org/10.1039/d1ee01642c.
[26] Qian Q, Luo Z, Sun H, Wei Q, Shi J, Li L. Life cycle assessment and techno-economic analysis of wood-based biorefineries for cellulosic ethanol production. Bioresour Technol 2024;399:130595. https://doi.org/10.1016/j.biortech.2024.130595.
[27] Qian Q, Luo Z, Sun H, Wei Q, Shi J, Li L, et al. Process evaluation of simulated novel cellulosic ethanol biorefineries coupled with lignin thermochemical conversion. Renew Energy 2024;231:120965. https://doi.org/10.1016/j.renene.2024.120965.
[28] Liu F, Dong X, Zhao X, Wang L. Life cycle assessment of organosolv biorefinery designs with the complete use of biomass. Energy Convers Manag 2021;246:114653. https://doi.org/10.1016/j.enconman.2021.114653.
[29] Tschulkow M, Pizzol M, Compernolle T, Van den Bosch S, Sels B, Van Passel S. The environmental impacts of the lignin-first biorefineries: a consequential life cycle assessment approach. Resour Conserv Recycl 2024;204:107466. https://doi.org/10.1016/j.resconrec.2024.107466.
[30] Luo Y, O'Dea RM, Gupta Y, Chang J, Sadula S, Soh LP, et al. A life cycle greenhouse gas model of a yellow poplar forest residue reductive catalytic fractionation biorefinery. Environ Eng Sci 2022;39(10):821–33. https://doi.org/10.1089/ees.2021.0472.
[31] Dominguez Aldama D, Grassauer F, Zhu Y, Ardestani-Jaafari A, Pelletier N. Allocation methods in life cycle assessments (LCAs) of agri-food co-products and food waste valorization systems: systematic review and recommendations. J Clean Prod 2023;421:138488. https://doi.org/10.1016/j.jclepro.2023.138488.
[32] Yu P, Fang M, Ma S, Cen J, Luo Z. Quantitative evaluation of coupling effects of pore structures and metal loadings on catalytic hydrogenation of tar model reactants over sulfided NiMo/γ-Al2O3 catalysts: role of segmented catalytic active phase volumes. Fuel Process Technol 2021;224:107008. https://doi.org/10.1016/j.fuproc.2021.107008.
[33] Muangsuwan C, Kriprasertkul W, Ratchahat S, Liu C-G, Posoknistakul P, Laosiripojana N, et al. Upgrading of light bio-oil from solvothermolysis liquefaction of an oil palm empty fruit bunch in glycerol by catalytic hydrodeoxygenation using NiMo/Al2O3 or CoMo/Al2O3 catalysts. ACS Omega 2021;6(4):2999–3016. https://doi.org/10.1021/acsomega.0c05387.
[34] Garbarino G, Riani P, Magistri L, Busca G. A study of the methanation of carbon dioxide on Ni/Al2O3 catalysts at atmospheric pressure. Int J Hydrogen Energy 2014;39(22):11557–65. https://doi.org/10.1016/j.ijhydene.2014.05.111.
[35] Liu Z, Han W, Hu D, Sun S, Hu A, Wang Z, et al. Effects of Ni–Al2O3 interaction on NiMo/Al2O3 hydrodesulfurization catalysts. J Catal 2020;387:62–72. https://doi.org/10.1016/j.jcat.2020.04.008.
[36] Chen M, Dai W, Wang Y, Tang Z, Li H, Li C, et al. Selective catalytic depolymerization of lignin to guaiacols over Mo-Mn/sepiolite in supercritical ethanol. Fuel 2023;333:126365. https://doi.org/10.1016/j.fuel.2022.126365.
[37] Phan D-P, Vo TK, Le VN, Kim J, Lee EY. Spray pyrolysis synthesis of bimetallic NiMo/Al2O3–TiO2 catalyst for hydrodeoxygenation of guaiacol: effects of bimetallic composition and reduction temperature. J Ind Eng Chem 2020;83:351–8. https://doi.org/10.1016/j.jiec.2019.12.008.
[38] Miao F, Luo Z, Zhou Q, Du L, Zhu W, Wang K, et al. Study on the reaction mechanism of C8+ aliphatic hydrocarbons obtained directly from biomass by hydropyrolysis vapor upgrading. Chem Eng J 2023;464. https://doi.org/10.1016/j.cej.2023.142639.
[39] Ma X, Ma R, Hao W, Chen M, Yan F, Cui K, et al. Common pathways in ethanolysis of kraft lignin to platform chemicals over molybdenum-based catalysts. ACS Catal 2015;5(8):4803–13. https://doi.org/10.1021/acscatal.5b01159.
[40] Cooreman E, Nicolaï T, Arts W, Aelst KV, Vangeel T, den Bosch SV, et al. The future biorefinery: the impact of upscaling the reductive catalytic fractionation of lignocellulose biomass on the quality of the lignin oil, carbohydrate products, and pulp. ACS Sustainable Chem Eng 2023. https://doi.org/10.1021/acssuschemeng.2c06913.
[41] Kubička D, Kaluža L. Deoxygenation of vegetable oils over sulfided Ni, Mo and NiMo catalysts. Appl Catal, A 2010;372(2):199–208. https://doi.org/10.1016/j.apcata.2009.10.034.
[42] Chen M, Lu H, Wang Y, Tang Z, Zhang J, Wang C, et al. Effect of reduction treatments of Mo/sepiolite catalyst on lignin depolymerization under supercritical ethanol. Energy Fuels 2020;34(3):3394–405. https://doi.org/10.1021/acs.energyfuels.9b04533.
[43] Chen M, Tang Z, Wang Y, Shi J, Li C, Yang Z, et al. Catalytic depolymerization of Kraft lignin to liquid fuels and guaiacol over phosphorus modified Mo/Sepiolite catalyst. Chem Eng J 2022;427:131761. https://doi.org/10.1016/j.cej.2021.131761.
[44] Hou M, Chen H, Li Y, Wang H, Zhang L, Bi Y. Reductive catalytic fractionation of lignocellulose over Ni/Al2O3 catalyst prepared by an EDTA-assisted impregnation method. Energy Fuels 2022;36:1929–38. https://doi.org/10.1021/acs.energyfuels.1c03923.
[45] Li X, Liu Y, Wang W, Wang J, Alorku K, Liu Q, et al. Effect of solvent systems on the synergistic catalytic hydrogenolysis of alkaline lignin over Pd/C-NaOH. Fuel 2023;349:128570. https://doi.org/10.1016/j.fuel.2023.128570.
[46] Jitpinit S, Chisti Y, Rattanasak U, Rakmak N, Nuithitikul K. Hydrothermal liquefaction of oil-palm-derived lignin to bio-oils for use as antioxidants in biodiesel. J Ind Eng Chem 2024;135:243–56. https://doi.org/10.1016/j.jiec.2024.01.036.
[47] Azadfar M, Gao AH, Bule MV, Chen S. Structural characterization of lignin: a potential source of antioxidants guaiacol and 4-vinylguaiacol. Int J Biol Macromol 2015;75:58–66. https://doi.org/10.1016/j.ijbiomac.2014.12.049.
[48] Dong L, Xia J, Guo Y, Liu X, Wang H, Wang Y. Mechanisms of Caromatic-C bonds cleavage in lignin over NbOx-supported Ru catalyst. J Catal 2021;394:94–103. https://doi.org/10.1016/j.jcat.2021.01.001.
[49] Liao Y, Koelewijn S-F, Van den Bossche G, Van Aelst J, Van den Bosch S, Renders T, et al. A sustainable wood biorefinery for low–carbon footprint chemicals production. Science 2020;367:1385–90. https://doi.org/10.1126/science.aau1567.
[50] Pan Z, Li Y, Wang B, Sun F, Xu F, Zhang X. Mild fractionation of poplar into reactive lignin via lignin-first strategy and its enhancement on cellulose saccharification. Bioresour Technol 2022;343:126122. https://doi.org/10.1016/j.biortech.2021.126122.
[51] Shao Y, Li C, Fan M, Gao G, Inkoua S, Zhang L, et al. Sequential pyrolysis for understanding specific influence of cellulose- and lignin-derived volatiles on properties of counterpart char. Green Chem Eng 2023;5:222–35. https://doi.org/10.1016/j.gce.2023.04.004.
[52] Xia T, Gong W, Chen Y, Duan M, Ma J, Cui X, et al. Sunlight-driven highly selective catalytic oxidation of 5-hydroxymethylfurfural towards tunable products. Angew Chem Int Ed 2022;61(29):1–6. https://doi.org/10.1002/anie.202204225.
[53] Jężak S, Dzida M, Zorębski M. High pressure physicochemical properties of 2-methylfuran and 2,5-dimethylfuran – second generation biofuels. Fuel 2016;184:334–43. https://doi.org/10.1016/j.fuel.2016.07.025.
[54] Tuan Hoang A, Viet Pham V. 2-Methylfuran (MF) as a potential biofuel: a thorough review on the production pathway from biomass, combustion progress, and application in engines. Renew Sustain Energy Rev 2021;148:111265. https://doi.org/10.1016/j.rser.2021.111265.
[55] Patil V, Singh P, Sonage S, Kumbhakarna N, Kumar S. Applicability of ketone-gasoline blended fuels for spark ignition engine through energy-exergy analyses. Fuel 2023;339:127416. https://doi.org/10.1016/j.fuel.2023.127416.
[56] Liu D, Giri BR, Farooq A. Cyclic ketones as future fuels: reactivity with OH radicals. J Phys Chem A 2019;123(20):4325–32. https://doi.org/10.1021/acs.jpca.9b00691.
[57] Wang L, Yin J, Jiang J, Zhang Y, Song M, Zhang R, et al. Revealing G-lignin model compounds pyrolysis behavior: β-O-4 and 5-5′ dimer and trimer. Fuel 2022;317:123531. https://doi.org/10.1016/j.fuel.2022.123531.
[58] Al-Rumaihi A, Shahbaz M, McKay G, Mackey H, Al-Ansari T. A review of pyrolysis technologies and feedstock: a blending approach for plastic and biomass towards optimum biochar yield. Renew Sustain Energy Rev 2022;167:112715. https://doi.org/10.1016/j.rser.2022.112715.
[59] Akhtar J, Saidina Amin N. A review on operating parameters for optimum liquid oil yield in biomass pyrolysis. Renew Sustain Energy Rev 2012;16(7):5101–9. https://doi.org/10.1016/j.rser.2012.05.033.
[60] Jang JH, Brandner DG, Dreiling RJ, Ringsby AJ, Bussard JR, Stanley LM, et al. Multi-pass flow-through reductive catalytic fractionation. Joule 2022;6:1–17. https://doi.org/10.1016/j.joule.2022.06.016.
[61] Li W, Ghosh A, Bbosa D, Brown R, Wright MM. Comparative techno-economic, uncertainty and life cycle analysis of lignocellulosic biomass solvent liquefaction and sugar fermentation to ethanol. ACS Sustainable Chem Eng 2018;6(12):16515–24. https://doi.org/10.1021/acssuschemeng.8b03622.
[62] Kulas D, Winjobi O, Zhou W, Shonnard D. Effects of coproduct uses on environmental and economic sustainability of hydrocarbon biofuel from one- and two-step pyrolysis of poplar. ACS Sustainable Chem Eng 2018;6(5):5969–80. https://doi.org/10.1021/acssuschemeng.7b04390.
[63] Van den Bosch S, Schutyser W, Vanholme R, Driessen T, Koelewijn SF, Renders T, et al. Reductive lignocellulose fractionation into soluble lignin-derived phenolic monomers and dimers and processable carbohydrate pulps. Energy Environ Sci 2015;8(6):1748–63. https://doi.org/10.1039/c5ee00204d.
[64] Sun H, Luo Z, Li S, Xue S, Zhou Q, Wei T, et al. Comparative life cycle assessment (LCA) of biofuel production via corn stover: fermentation to ethanol, pyrolysis to bio-oil, and gasification to jet fuel. Biomass Convers Biorefin 2021;13:12809–21. https://doi.org/10.1007/s13399-021-02054-z.